Annual Review of Analytical Chemistry

(Multi)functional Atomic Force Microscopy Imaging

Anisha N. Patel and Christine Kranz

Institute of Analytical and Bioanalytical Chemistry, Ulm University, Ulm 89081, Germany; email: christine.kranz@uni-ulm.de

Annu. Rev. Anal. Chem. 2018. 11:329–50

First published as a Review in Advance on February 28, 2018

The *Annual Review of Analytical Chemistry* is online at anchem.annualreviews.org

https://doi.org/10.1146/annurev-anchem-061417-125716

Keywords

multiparametric AFM, molecular recognition imaging, AFM probe modification, atomic force microscopy–scanning electrochemical microscopy

Abstract

Incorporating functionality to atomic force microscopy (AFM) to obtain physical and chemical information has always been a strong focus in AFM research. Modifying AFM probes with specific molecules permits accessibility of chemical information via specific reactions and interactions. Fundamental understanding of molecular processes at the solid/liquid interface with high spatial resolution is essential to many emerging research areas. Nanoscale electrochemical imaging has emerged as a complementary technique to advanced AFM techniques, providing information on electrochemical interfacial processes. While this review presents a brief introduction to advanced AFM imaging modes, such as multiparametric AFM and topography recognition imaging, the main focus herein is on electrochemical imaging via hybrid AFM-scanning electrochemical microscopy. Recent applications and the challenges associated with such nanoelectrochemical imaging strategies are presented.

1. INTRODUCTION

Atomic force microscopy (AFM) is one of the most widespread scanning probe microscopy (SPM) techniques. AFM is based on determining short- and long-range force interactions between the AFM tip (i.e., the typical curvature radius of several nanometers) located at the end of a cantilever and the sample surface. A feedback loop maintains either a constant cantilever deflection, where short-range forces dominate, or a constant cantilever amplitude (i.e., dynamic mode).

Fundamental research on AFM technology remains active and addresses such areas as imaging speed (i.e., video rate AFM), molecular recognition (i.e., identification of chemical structures of single molecules), multifrequency imaging, as well as hybrid techniques with various spectroscopies, high-resolution optical microscopy, or complementary scanning probe techniques, including scanning electrochemical microscopy (SECM) (1). AFM matured shortly after its introduction in 1986 (2) into the most commonly used SPM technique due to its versatility, the multitude of force interactions that can be studied (e.g., magnetic, electrostatic, and thermal properties), and the wide variety of samples that can be studied independent of their surface properties (e.g., softness, conductivity). Furthermore, AFM measurements can be performed in vacuum, at ambient atmospheric conditions, and in solution, including (biological) buffers. The early availability of well-defined microfabricated AFM cantilevers, with force constants ranging from 0.01 N/m up to 100 N/m, has contributed to its widespread applications. However, the "chemical blindness" of conventional AFM measurements always sparked significant interest to overcome this limitation. To obtain chemical or electrochemical information, the AFM probe, typically composed of silicon, silicon nitride, or silicon oxide tip, has to be modified. **Figure 1** presents an overview of functionalized AFM probes used under different experimental conditions that all provide chemical information. Such modifications frequently entail the covalent attachment of specific recognition or capture molecules to the AFM probe. Specific

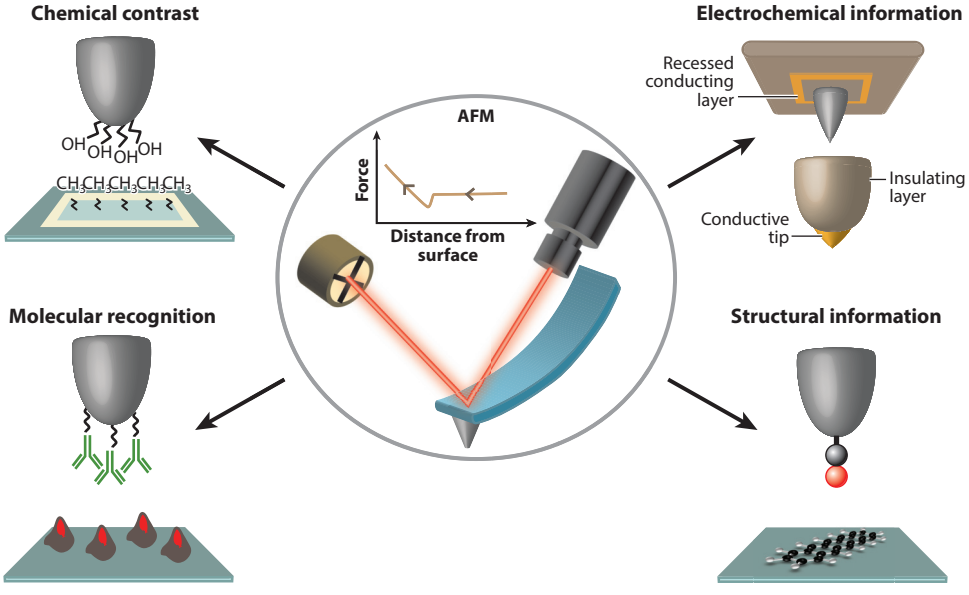

Figure 1

Schematic representation of various chemical atomic force microscopy (AFM) imaging approaches based on modified AFM probes either by attaching functional groups and molecules or by integrating an electrode into the AFM probe.

force interactions between the tip-bound molecules and molecules at the sample surface can be quantitatively determined. This approach is used for measuring binding forces, as first shown by Gaub and coworkers for avidin/streptavidin (3). In the same year, Frisbie et al. (4) demonstrated chemical imaging in ethanolic solution based on friction and adhesion changes between a functionalized gold-coated AFM probe and a lithographically patterned sample surface. The tip and sample were modified with self-assembled monolayers bearing carboxylic, methyl, or amino groups at the end of the alkyl chain. Hydrogen bonding, dipole–dipole interactions, and hydrophobic interactions between $-COOH$, $-CH_3$, and $-NH_3$ groups of the modified AFM probe and the sample surface were monitored by contrast in the friction image. The measured adhesive forces agreed well with theory (5).

Gross and coworkers at IBM (6) demonstrated atomic resolution of individual molecules with carbon monoxide–modified probes in noncontact mode at high vacuum conditions. Chemical structures of natural compounds such as cephalandole A could be finally determined by combining the data of the AFM measurements with density functional theory simulations, nuclear magnetic resonance, and mass spectrometry data (7). Molecular recognition imaging, which can be performed in air or in a liquid environment, provides two-dimensional (2D) topographical maps of specific molecular interactions using an appropriately modified AFM probe. It should be noted that such molecular-specific imaging techniques are highly valuable (8–11); yet, they have thus far only been applied by a fairly small group of researchers who are usually experts in this field. In addition, most interfacial processes, relevant not only to biomedical research but also to catalysis, corrosion science, and energy-related topics, involve electrochemical processes at the solid/liquid interface. In particular, spatially resolved electrochemical information, which may be correlated to structural features or interfacial changes due to degradation and structural rearrangements during electrochemical reactions, is relevant in many emerging areas. Hence, this review mainly focuses on advances in AFM-SECM technology, highlighting recent developments and applications within a variety of research areas. Additionally, it briefly discusses multiparametric AFM imaging based on functionalized AFM probes, which is widely used in biophysics and biomedically related research. In-depth information can be found in recently published review articles (11–13).

2. MULTIPARAMETRIC ATOMIC FORCE MICROSCOPY IMAGING VIA FUNCTIONALIZED CANTILEVERS

Due to the high force sensitivity ranging from 10 to 10^6 pN (14), AFM is employed to record force-distance (FD) curves, providing a breadth of information on tip–sample interaction, such as adhesion, elasticity, and energy dissipation (15). In terms of proteins and polymers, information on unfolding events may be obtained (16). Force-based imaging is considered to exceed the performance of more conventional modes of AFM for measuring and mapping mechanical properties and biological interactions. Significant developments in instrumentation have improved acquisition speed, enabling force-based imaging AFM modes, e.g., quantitative nanomechanical mapping, as marketed by the Bruker Corporation as PeakForce Tapping™ (PFT) mode (17), which is similar to pulsed-force mode (18) and force-volume imaging (19, 20). FD-based imaging is also termed multiparametric AFM (13). Multiparametric imaging employs AFM tips functionalized with a specific chemical group, e.g., a ligand or antibody, to map specific interactions with the biological sample. When the modified probe is brought to the sample surface, a specific binding event may occur. When the AFM tip is retracted, it reflects an increasing force to this bond (e.g., ligand-receptor bond) that dissociates at a critical force. This provides information on the localization of the receptor but also on binding constants, which can be measured in real time with topography. Examples of different applications include mapping specific binding sites (21),

correlating the structure and assembly of soluble proteins (22), measuring the kinetics and thermodynamics of ligand-receptor interactions (23), monitoring assembly and binding events of viruses (24), and determining cell adhesion (25). As an example, Dufrêne and coworkers (26) demonstrated FD-based AFM imaging to correlate the structure of filamentous bacteriophages extruding from living bacteria with their biophysical properties. Using a nickel-functionalized AFM tip to detect histidine tags, they showed that the structure, adhesion, and elasticity of infected bacteria can be mapped and that the sites of assembly and extrusion form soft nanodomains surrounded by stiff cell wall material.

2.1. Functionalization of Atomic Force Microscopy Probes

Given the high force sensitivity of AFM, binding forces between single entities can be quantitatively determined. Specifically, functionalized probes are required for using FD curves to detect molecular interactions. Statistically meaningful force measurements require well-defined and reproducible modification of the AFM probe. AFM probes can be easily modified through silanization in the case of silicon, silicon nitride, and silicon oxide probes. The modification process is usually a multistep process dependent on the AFM probe material. For example, to functionalize silicon or silicon-nitride AFM probes, the tip is first silanized with a short-chain silane such as (3-aminopropyl)triethoxysilane, which is then typically cross-linked with a functional and relatively long polyethylene glycol (PEG) linker, to which the ligand of interest can be attached (see **Figure 2*a***) (27). PEG is commonly used because of its conformational flexibility.

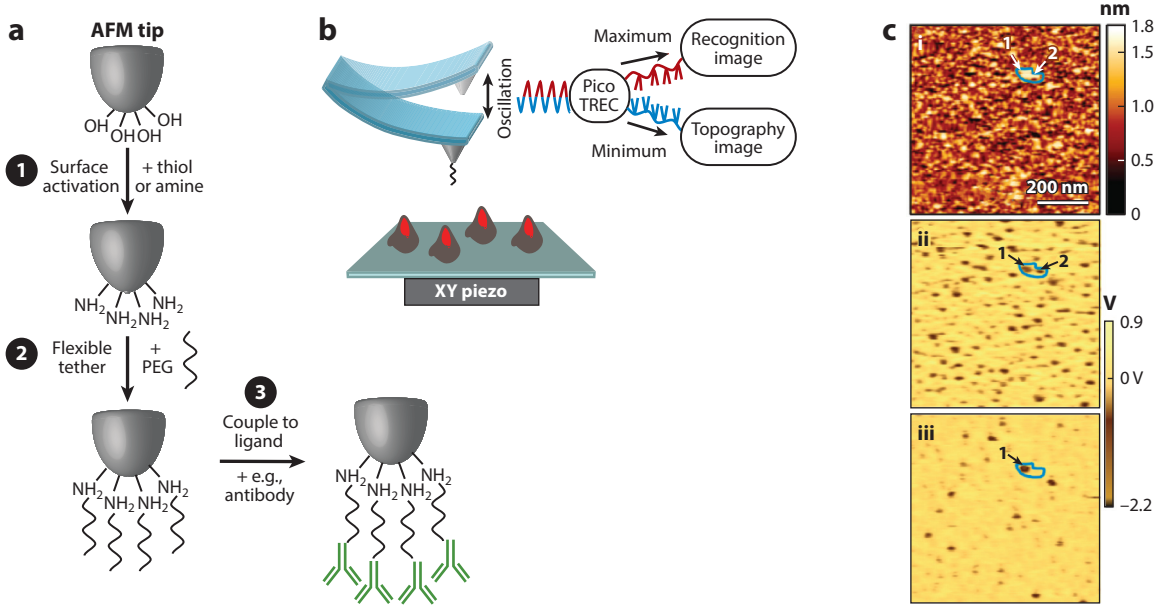

Figure 2

(*a*) Modification steps for covalent attachment of biomolecules. (*b*) Schematic view of separating the maxima and minima of the oscillation amplitude. (*c*) Topographic (*i*) and recognition (*ii*) image of a VEGF and TNF-α mixture; the areas marked in green reflect spots with proteins (*i*), which can be identified as two protein molecules in the recognition image (*ii*); (*iii*) the anti-VEGF aptamer-blocked recognition image with the green marked area corresponds to TNF-α. Panel *c* adapted with permission from Reference 28. Copyright 2015, American Chemical Society. Abbreviations: AFM, atomic force microscopy; PEG, polyethylene glycol; TNF-α, tumor necrosis factor-alpha; TREC, topography and recognition imaging; VEGF, vascular endothelial growth factor.

For multiplex molecular interactions, the AFM probes are also functionalized with a heterofunctional three-arm linker to conjugate two different molecules using a catalyst-free click reaction (28).

Alternatively, the AFM probe can be coated with a thin (several nanometers thick) gold layer, which can then be easily modified with an alkanethiol monolayer that is terminated by specific functional groups for linking the ligand of interest (29–32). Bifunctional AFM-SECM probes with the electrochemical area at the tip apex have been similarly modified with PEG groups bearing a redox molecule as the functional group (33).

2.2. Topography and Recognition Imaging

Topography and recognition imaging (TREC) is a force spectroscopy–based imaging technique that simultaneously performs dynamic force mapping and topographical imaging (34). The AFM tip is modified with recognition molecules by smart linker chemistry and then scanned in dynamic mode across the sample surface. This brings the ligand through a long spacer into contact with the surface containing the respective cognate receptors, leading to ligand-receptor bonding. The relatively long spacer acts as a nanospring so that nonspecific force interactions with the body of the AFM probe are omitted. In principle, the oscillation characteristics of the AFM probe contain the topographical information in the deflection signal minima, reflecting the decrease in amplitude when the probe gets in contact with the sample surface. In case of a binding event, the oscillation amplitude maxima are modulated, as the oscillating tip cannot return to its original position due to the acting binding force. Using appropriate electronic circuits and software as offered by Keysight Technologies (PicoTREC™) allows the maxima and minima of the oscillation amplitude to be separated and independently evaluated, as shown in **Figure 2*b***, resulting in the topography and recognition images, respectively.

Simultaneously obtained recognition and topography maps are superimposed to obtain extremely accurate maps of the protein locations in the topographic images. Using a magnetically driven cantilever (35), Raab et al. (36) showed TREC imaging by covalently linking antibodies to a PEG-modified AFM tip to obtain a 2D map of a lysozyme immobilized on a mica surface. Molecular recognition imaging has been employed to map the interactions between aptamer and protein (37), peptide and protein (38), antigen and antibody (39), and RNA or DNA strands with cells (37, 38); it also maps antibody and chromatin binding (40) and aptamer-histone proteins (41).

3. ATOMIC FORCE MICROSCOPY-SCANNING ELECTROCHEMICAL MICROSCOPY

SECM is a noninvasive and noncontact electrochemical SPM technique introduced by Bard and coworkers (42), from which laterally resolved information on surface processes and at liquid/liquid interfaces can be obtained. This technique has led to applications in multidisciplinary research areas ranging from biomedical research to materials science, corrosion, and catalysis, as well as in energy-related topics, such as photocatalysis, fuel cells, and battery research (43). Recently, SECM has experienced a quantum leap toward nanoscale imaging (44, 45), yet it demands a well-defined and well-controlled distance of the nanosized SECM probe to the sample surface to avoid erroneous information. Several approaches have been successfully developed to achieve constant-distance SECM; these include shear force mode positioning of the probe (46, 47), SECM combined with SPM techniques that facilitate positioning of the nanosized electrode (e.g., combined AFM-SECM), scanning ion conductance microscopy (SICM)-SECM using

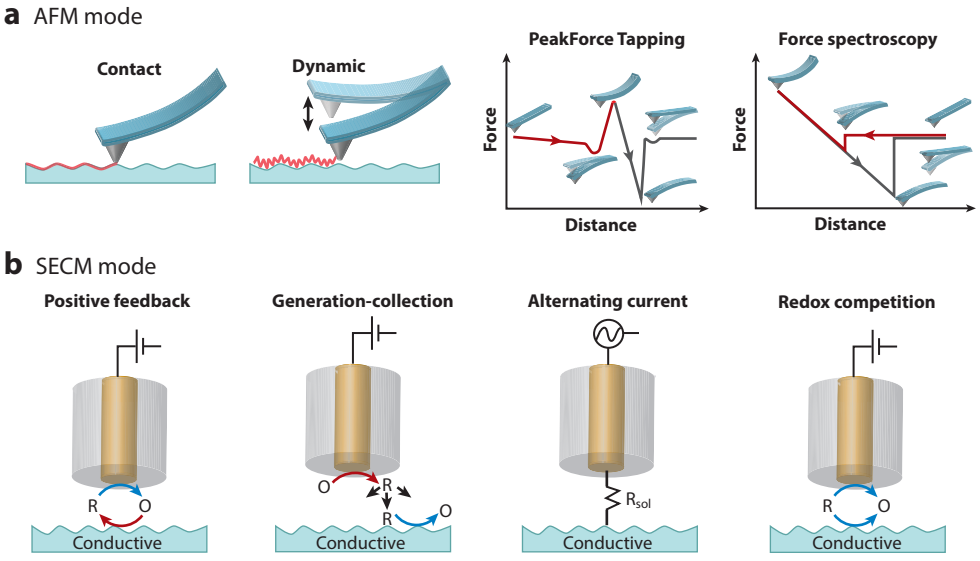

Figure 3

AFM imaging modes for measurements in ambient conditions and in solution. (*a*, *left to right*) In contact mode, there is permanent contact of the AFM tip with the sample surface. In dynamic mode (also known as intermittent contact mode, tapping mode, or acoustically driven mode), the AFM cantilever is oscillated at a frequency below its resonance frequency, and the tip is in brief contact at the lower oscillation part with the sample surface. With PeakForce Tapping, a force curve is recorded at each pixel. The feedback loop enables control of the applied force at low values (down to 10 pN). In force spectroscopy, force-distance curves are recorded that contain information on physical sample properties. (*b*) SECM imaging experiments are predominantly performed in feedback mode with an artificial redox mediator added to solution. In mode, redox-active molecules generated at the surface are collected at the SECM probe; alternatively, tip-generated species can be detected on a conductive sample surface. AC mode is based on superimposing an AC voltage signal to a small DC voltage at the SECM tip; the measured current magnitude and phase angle response are dependent on the nature of the sample surface. In redox competition mode, the SECM probe and the sample compete for the same electroactive species. The tip current is reduced if areas of high activity on the sample are scanned. Abbreviations: AC, alternate current; AFM, atomic force microscopy; DC, direct current; R_{sol}, solution resistance; SECM, scanning electrochemical microscopy.

bifunctional theta pipette–based probes (48), or alternatively, pipettes modified with a ring electrode (49). Recently, scanning electrochemical cell microscopy (SECCM), which has been described in depth in several recent reviews, has emerged as a powerful tool for electrochemical imaging with high spatial and temporal resolution (45, 50).

In contrast to these electrochemical scanning probe techniques, the method of adding electrochemical functionality to the AFM probe provides superior spatial resolution in terms of surface topology and (nano)mechanical information inherent to AFM, whereas the integrated SECM functionality gives nanoscale electrochemical information that is directly and inherently correlated to the sample topography. In addition, the distance between sample and electrode can be precisely determined with the accurate positioning of the AFM tip. The core advantage of combined AFM-SECM is that the well-established imaging modes of each technique, as schematically shown in **Figure 3**, are readily combined and may be tailored toward the targeted application and desired surface information.

Initial AFM-SECM measurements were demonstrated in AFM contact mode and SECM feedback mode by Macpherson & Unwin (51). To bypass electrical shorting problems when conductive substrates (i.e. electrodes) were imaged, they implemented a two-pass technique: For each scanned line, the sample topography was mapped in the first pass, and electrochemical data were collected in the second pass (52). This so-called lift mode remains popular for combined measurements using AFM-SECM probes with the electroactive area at the tip apex. In contrast, probes with the electroactive area located at a certain distance recessed from the tip apex (i.e., the AFM tip itself remains insulating) may be used for simultaneously recording both sets of information independent of the nature of the sample surface (53). Dynamic AFM modes are required when imaging soft samples such as hydrophilic polymers or biological specimens (e.g., cells, microbes). Recently, combined measurements have also been demonstrated in PFT (17), which provide information on nanomechanical properties and can be further combined with electrochemical information (54). In respect to SECM measurements, experiments have been performed in generation-collection mode for surface patterning (55), pitting experiments (56), corrosion studies (57), and growth and dissolution studies (58, 59). In addition, experiments in alternating current (AC) mode have been performed (60, 61); this method has some similarity to electrochemical impedance spectroscopy, as the magnitude of the tip current and the phase angle are obtained by their dependence on the AC potential applied to the AFM-SECM probe. An advantage of AC-mode imaging is that a redox mediator is not required. However, it should be noted that typical experiments are performed using micrometer-sized electrodes to achieve sufficient signal contrast. For that purpose, batch-fabricated AFM-SECM probes bearing a microsized ring platinum electrode were used in these experiments (62). Although combined AFM-SECM measurements have not yet been performed in the redox competition mode of SECM (63), this technique may have significant potential for future applications in catalysis. It should be noted that force spectroscopy combined with the simultaneously recorded current distance curves provides the basis for a quantitative evaluation of physical and electrochemical parameters, such as adhesion forces, and the determination of apparent electron-transfer rate constants.

Instrumentally speaking, AFM-SECM is rather straightforward, as an external (bi)potentiostat may be used to control the electrochemical experiment. The electrochemical data can then be fed in via an available analog-to-digital conversion channel provided by any AFM controller. Mounting and electrical contact of the AFM-SECM probe require modification of the AFM chip holder. Special care is required for the insulation of the conductive area, as the entire AFM chip will be immersed in solution during AFM-SECM experiments. However, most post-applied insulating varnishes or UV curable glues have limited stability at extreme pH. In addition, electrochemical control with an external (bi)potentiostat requires fairly long cable connections to the AFM-SECM probe, resulting in unfavorable signal-to-noise ratios due to parasitic couplings. To avoid this, AFM chip mounts with integrated amplifiers promise significant improvements in the signal-to-noise ratio. Almost all commercial AFM systems use an optical readout mechanism for detecting the movement of the cantilever (e.g., deflection, friction), which can also be used for AFM-SECM probes. Recently, tuning fork–based noncontact AFM was successfully used for AFM-SECM experiments (64). The high stiffness of the tuning fork allows noncontact operation with small oscillation of the tip (<1 nm).

SECM functionality only recently became commercially available as an add-on to AFM instruments from Keysight Technologies (65) and the Bruker Corporation (66). Similar to TREC, AFM-SECM was to date mainly used by a small group of experienced researchers. Whether this technique will also find more widespread application in routine scenarios is certainly dependent on the availability, reproducibility, and integrity of bifunctional probes. In the next section, probe designs along with their specific advantages and disadvantages are discussed.

3.1. Atomic Force Microscopy-Scanning Electrochemical Microscopy Probe Design

The reliability of the recorded data and the achievable resolution in AFM-SECM experiments are predominantly determined by the bifunctional AFM-SECM probe. Several designs of probes have been developed and can be divided in two main groups: (*a*) AFM-SECM probes with a conductive apex, i.e., mostly a conically electrode; and (*b*) AFM-SECM probes where the electrode is located at a certain distance (dependent on the active electrode size) recessed from the nonconductive tip apex. AFM-SECM probes can also be categorized by the fabrication method, as probes are either fabricated manually based on etching and bending wires (cantilever-shaped electrodes) (51, 67) or produced using standard microfabrication techniques (53, 68–70), including standard deposition processes, electron beam lithography, and focused ion beam milling. Shin et al. (62) presented a standard batch fabrication process, which can be entirely performed at a wafer-batch level; however, the integrated platinum ring electrodes have diameters in the micrometer region. **Figure 4** schematically shows the different probe designs along with scanning electron microscope (SEM) images visualizing various designs.

Despite the preferred design for the targeted application, pinhole-free insulation of the AFM-SECM (except for the submicrosized or nanosized electroactive area) and the insulation of the electrical connecting part are the most critical features for avoiding any leakage currents that may lead to erroneous electrochemical information. Microfabricated probes are mostly insulated with layers of silicon nitride or mixed layers of silicon oxide and silicon nitride deposited via plasma-enhanced chemical vapor deposition. One issue for soft silicon nitride cantilevers is tensile stress, which may lead to an undesirable bending of the cantilever. However, controlling the thickness and sequence of the layers along with optimizing deposition conditions allows the deposition of an insulation layer with a total thickness of 1–1.5 μm with a maximum of 1–2° bending of the cantilever. Alternatively, Parylene C has been used for insulating microfabricated (72) and commercially available conductive AFM probes (73). Parylene C forms stress-free, conformal, pinhole-free films with high dielectric strength and approved biocompatibility. In addition, the change in force constant of the Parylene C–coated cantilever is minimal, which is required for sensitive force measurements and is less compared to silicon nitride, where the coating results in a change of almost 1 N/m. Furthermore, intrinsic oxygen-terminated diamond may be an interesting material, especially if the electrode material is boron-doped diamond for targeted applications in a harsh chemical environment. The insulation of bench top–fabricated cantilever-shaped etched microwires is obtained with epoxy (74) but mostly via so-called electrophoretic paints (51). These can be electrodeposited and may shrink during the heat-induced cross-linking process, thereby exposing a conical electrode at the tip apex. In contrast to nanoelectrodes based on pipettes, where graphitic carbon is the predominant electrode material, gold and platinum are the preferred electrode materials for AFM-SECM probes independent of the probe design. Eifert et al. (75, 76) also optimized and thoroughly studied boron-doped diamond as an electrode material for AFM-SECM probes, which is interesting given the large potential window and the physical and chemical inertness. Focused ion beam–induced deposition of carbon/platinum has been employed either to enlarge the electroactive area of the tip-integrated electrode (77) or to fabricate a conical electrode at the tip apex (78). Next to a conical electrode shape, a disc, ring, and frame shape have been realized, depending on the fabrication process. Disc electrodes have been fabricated down to a dimension of an approximately 50-nm electrode radius, which enables high-resolution electrochemical imaging (79).

Bench-top fabrication does not require cleanroom facilities, which makes this approach attractive for researchers. However, controlling and maintaining relevant parameters such as force constant and tip curvature radius among individually fabricated probes remain challenging compared

to microfabricated probes, in which the fabrication process inherently determines the physical parameters at a batch level. Variation of the exposed spherical and conical electrodes with radii ranging from 150 to 550 nm was reported by Abbou et al. (67), which was improved to 20–100 nm as later reported by the same group (80). Macpherson & Unwin (51) reported effective tip radii ranging from 50 nm to 2.5 μm within a batch of 50 fabricated tips.

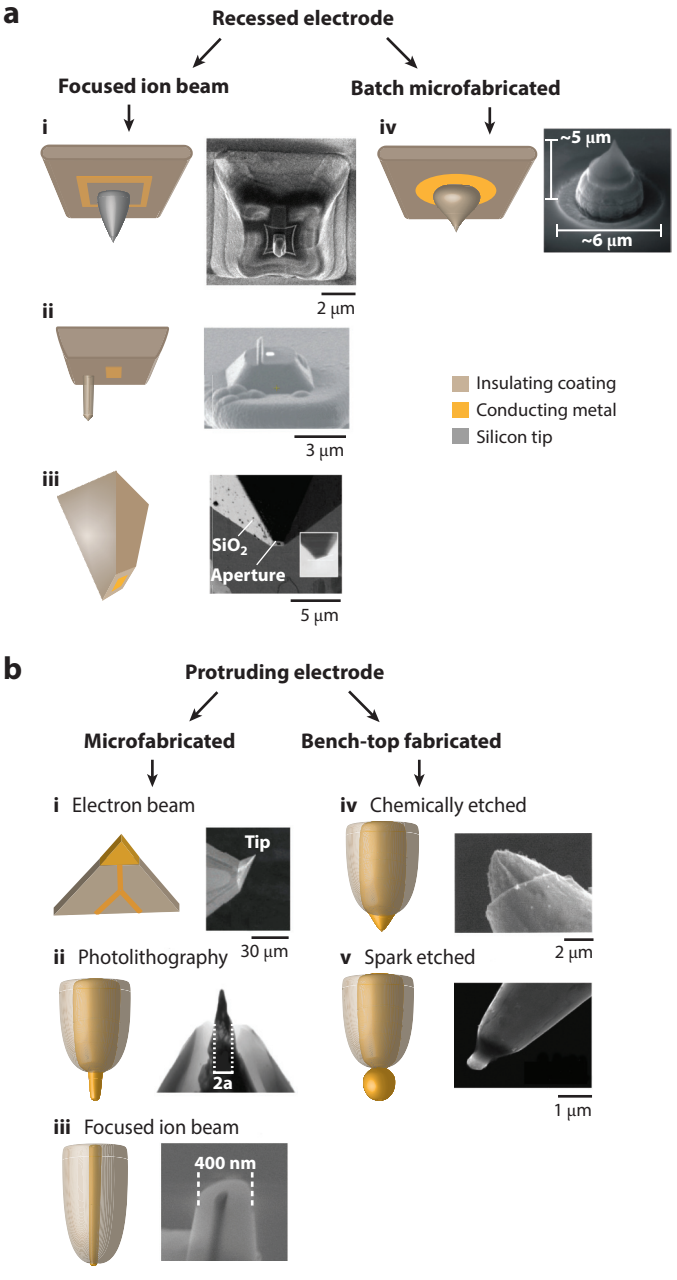

(*Caption appears on following page*)

Figure 4 (*Figure appears on preceding page*)

(*a*) Scheme and SEM images of AFM-SECM probes with recessed electrodes. (*i*) Gold frame electrode, (*ii*) recessed disc electrode, (*iii*) gold disc nanoelectrode, and (*iv*) tip-integrated platinum ring electrode. The recessed location of the nanoelectrode (*iii*) is achieved by exposure of the electroactive area by focused ion beam milling at a certain angle that generates a tilt of the truncated pyramid. Adapted with permission from Reference 71. Copyright 2010, Elsevier. (*b*, *i–iii*) AFM-SECM probes with the electrode at the tip apex. (*i*) Triangular-shaped electrode. Adapted with permission from Reference 68. Copyright 2005, American Chemical Society. (*ii*) AFM tip-integrated conical platinum electrode. Adapted with permission from Reference 69. Copyright 2006, American Chemical Society. (*iii*) Focused ion beam–fabricated disc electrode. Adapted with permission from Reference 64. Copyright 2017, American Chemical Society. (*b*, *iv–v*) Bench top–fabricated probes. (*iv*) Cantilever-shaped conical platinum electrode. Adapted with permission from Reference 51. Copyright 2000, American Chemical Society. (*v*) Spherical gold electrode formed via a controlled arc discharge technique. Adapted with permission from Reference 67. Copyright 2002, American Chemical Society. Abbreviations: AFM, atomic force microscopy; SECM, scanning electrochemical microscopy; SEM, scanning electron microscope.

Finally, AFM-SECM probes are commercially available today with a conical platinum electrode at the AFM tip apex, as a needle-type platinum probe, and as probes with a nonconductive AFM tip and a gold electrode located at a defined distance from the tip.

3.2. Electrode Modification

The electroactive area of the AFM-SECM probe is modified when direct electrochemical detection of specific molecules is difficult (e.g., detection of biomedically relevant molecules in complex samples). With probe designs bearing the electroactive area at the tip apex, contact between the sample surface and the probe may affect coatings, thus leading to unreliable electrochemical information. Surface modifications also improve the achievable electrochemical resolution of combined AFM-SECM measurements, for example, for mapping nanosized objects in feedback mode. Ideally, the achievable spatial resolution of both techniques is on the same order of magnitude. However, in respect to SECM, there is a fundamental limitation to the spatial resolution in feedback-mode operation associated with the electron transfer kinetics. Sizeable turnover rates of the redox-active molecules are required to generate sufficient contrast in the electrochemical response (81). An elegant approach to overcome such limitations was introduced by Demaille and coworkers (82) by tethering redox-active molecules (e.g., ferrocene moieties) to the tip, thereby confining the diffusional dispersion. Anne et al. (33) introduced a mode called tip-attached redox mediator (Tarm)/AFM-SECM. Redox-active molecules are tethered to the electrode surface of the AFM-SECM probe using a flexible PEG cross-linker similar to the procedures described for modifying TREC AFM probes. The conductive features on the sample surface could be probed independently of their turnover rate of the redox-active molecule with a lateral resolution of 20–40 nm.

Miniaturized biosensors exhibit high molecular specificity as well as high sensitivity. Thus far, only AFM-SECM probes with recessed electrodes have been modified with enzyme-containing layers. The enzymes are entrapped within, for example, an electrochemically deposited membrane, thus confining the site of immobilization to the electrode surface. For this purpose, electrophoretic paints or polyphenoxazines are suitable matrices preserving the activity of the enzymes and ensuring a sufficient amount of molecules to be entrapped (83–86).

Kueng et al. (87) modified the gold frame electrode of an AFM-SECM probe with glucose oxidase using an anodic electrophoretic paint. The calibration of the tip-integrated biosensor toward glucose showed a linear range of up to 2 mM of glucose. The resulting biosensor AFM-SECM probe was tested by imaging the diffusion of glucose through an artificial membrane,

comprising pores with diameters of approximately 200 nm simultaneously with the topography in dynamic mode. Alternatively, enzymes can be immobilized on the electrode surface using self-assembled thiol monolayers with reactive headgroups, as demonstrated by the same researchers with the immobilization of horseradish peroxidase (88).

Conductive colloidal AFM-SECM probes represent a novel design that was recently introduced by Knittel et al. (89) and applied to single-cell force spectroscopy. An insulated tipless AFM-SECM probe with a small conductive recessed disc electrode at the end of the cantilever was modified with a gold-coated colloid, which was glued to the disc electrode. The colloidal probe could then be further modified via, for example, conductive polymer layers. Such probes are highly suitable for force spectroscopic measurements that study the effect of electrical signals on cellular and molecular interactions.

3.3. Theoretical Considerations

SECM is predominantly performed using disc-shaped microelectrodes, and well-established theoretical models are available predicting the current response in feedback and generation-collection mode. Thus so far, only a few studies have been dedicated to predicting the theoretical AFM-SECM probe response, which may be related to the more complex geometry of such probes. Finite element method (FEM) (68) and boundary element method (BEM) simulations (90) were used to model the response of triangular microelectrodes and frame-shaped recessed electrodes, respectively. BEM was also used to model theoretical approach curves and the current response of disc-shaped electrodes recessed from the tip apex that exhibit different geometries (91). Eifert et al. (76) developed an advanced software-controlled focused ion beam–based patterning process for semiautomated fabrication of AFM-SECM probes. As the milling process occurs from the top, the insulation material influences the overall probe geometry. Consequently, a tilt angle of the electrode toward either the outer or inner side is obtained, which influences the current response. Numerical simulations of the mass transport toward such tilted electrodes were performed using FEM modeling, via a commercial software package (COMSOL Multiphysics) (76). A top-mill–fabricated SixNy-coated probe with an inward-tilted electrode showed a significantly reduced diffusive flux toward the electrode, which could be experimentally confirmed by a decreased current response. Denuault and coworkers (92) used an FEM solver to model the response of a conically shaped electrode located at the center of a flat tip apex.

4. SELECTED APPLICATION AREAS

Almost two decades after the first reports on combined AFM-SECM, the technique has not quite reached the level of maturity required for routine measurements comparable to those obtained through conventional AFM. The high costs of the probes compared to standard AFM probes and their relatively recent commercialization may explain their limited usage. Furthermore, AFM probes, either conventional or bifunctional, are considered consumables. Hence, depending on the nature of the investigated samples, contamination or wear over a finite lifetime is unavoidable. In this respect, diamond-coated probes, which may also be functionalized with an electrode (93), are a particularly interesting strategy to overcome this limitation. Although it is evident that commercial suppliers have an interest in such probes (i.e., expensive probes) as consumables, reducing the costs of AFM-SECM probes would give the field a significant boost. Many publications concerning AFM-SECM are related to novel probe designs, instrumental improvements, and the application of various imaging modes such as electrochemical PFT. These applications are usually on model substrates, including structured conductive/nonconductive surfaces, artificial membranes, carbon materials such as highly ordered pyrolytic graphite (HOPG) and carbon

nanotubes, microelectrodes, and microelectrode arrays. In a positive trend, recent research has shown applications in or close to real-world sample scenarios, thus providing fundamental understanding of high practical value on interfacial processes at the nanoscale.

4.1. Corrosion and Energy-Related Materials

Investigation of corrosion processes was an early focus of AFM-SECM measurements. Localized corrosion processes on aluminum alloys have been studied in chloride- and iodide-containing solutions at micrometer electrochemical resolution, whereas morphological changes could be mapped (74, 94). Gaining fundamental insight into corrosion processes requires spatially resolved information on morphological changes associated with electrochemical processes occurring at the metal/liquid interface. Metallic corrosion involves micrometer- to nanometer-sized defects, which may form microgalvanic cells, and hence, initiate the onset of corrosion processes at the micro- and nanoscales known as pitting corrosion.

Izquierdo et al. (56, 59, 95, 96) recently showed a series of applications of AFM-SECM related to corrosion science. For example, they demonstrated the formation of corrosion pits on iron surfaces, which were protected by an iron nitrate layer. The recessed AFM tip-integrated frame electrode induced a local change in pH due to water splitting at the tip, which generated defects in the projection layer. As experiments were performed in a chloride-containing solution, the iron surface was attacked by the aggressive media, and depending on the duration and imaging mode (i.e., static or scanning), corrosion pits were formed, which could be monitored in situ by the AFM probe (56, 96). Corrosion processes on copper surfaces due to anodic dissolution in acidic chloride solution were presented by the same authors (59, 95). The dissolution of model copper-modified substrates (copper nanoparticles on gold) and bulk copper samples used in industrial settings has been investigated. Copper is one of the most widely used metals in industry, for example, in electronics and heat exchangers. AFM-SECM probes with recessed frame electrodes revealed topographical changes with submicrometer spatial resolution caused by corrosion processes in acidic chloride solution related to local passivation and pitting phenomena, as shown in **Figure 5**. A semiquantitative determination of the attack was estimated by anodic stripping of the copper metal deposited on the probe during such dissolution experiments. Moreover, the accumulation of corrosion products leading to local passivation on the copper surface could be correlated with the absence of copper cations over those sites. Quantitative surface roughness obtained via the AFM data allowed the characterization of initial growth and subsequent breakdown along with pit formation, whereas the accompanying progressive activation of the copper surface and Cu(II) release was locally detected by the AFM tip-integrated SECM electrode. In addition to its use in these corrosion studies, AFM-SECM has also been used to study the heterogeneous electrochemical activity of metallic alloys such as Ti-6Al-4V (91).

An emerging research field in which AFM-SECM may potentially play an important future role is energy-related studies. These include research on the formation of solid surface electrolyte interface (SEI) degradation, the passivation of anodes and cathodes, and the photocatalytic system for water splitting. To date, AFM-SECM has been rarely employed in such application scenarios. The first approaches go back to Macpherson and coworkers' (97) initial work using bench-top fabricated AFM-SECM probes to investigate Ti/TiO_2 anodes in respect to the electrochemical and structural properties. A sequential imaging approach involving AFM and SECM has been demonstrated by Zampardi et al. (98). An SPM platform housed in a glovebox allowed sequential electrochemical (EC)-AFM, AFM, and SECM measurements of the same sample in a sequential procedure (98). Within this approach, SEI grown on a glassy carbon sample induced by EC-AFM has been characterized first in terms of topography and then consecutively via SECM feedback mode. Recently, the interfacial properties of electroless Pt nanoparticles deposited on p-Si and

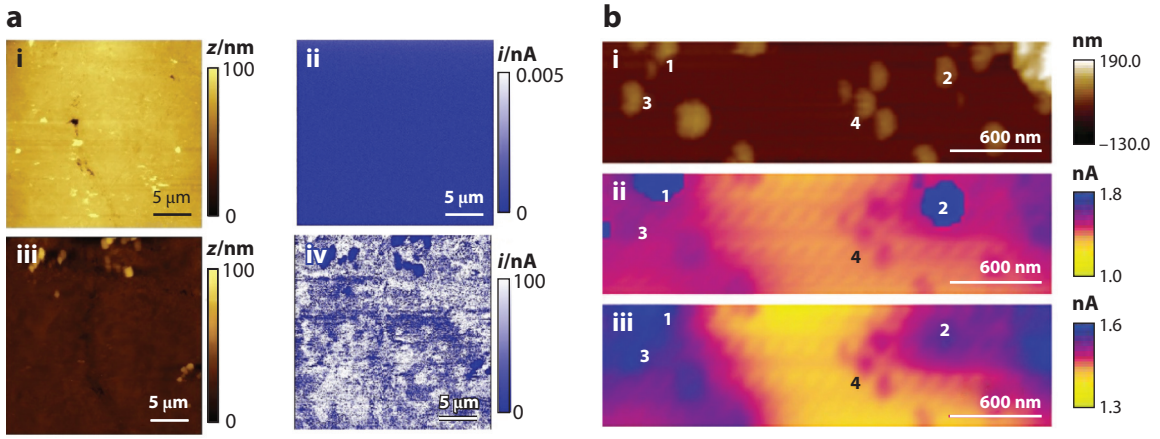

Figure 5

(*a*) AFM-SECM images of a copper substrate polarized at (*i*, *ii*) −0.35 and (*iii*, *iv*) −0.18 V versus Ag/AgCl in 0.5 M NaCl (pH = 3). Subpanels *i*, *iii* show substrate topography; subpanels *ii*, *iv* show tip current. The tip was biased at −0.45 V. Adapted with permission from Reference 95. Copyright 2017, Elsevier. (*b*) PFT-SECM imaging of Pt nanoparticles electrolessly deposited onto a degenerately doped p^+-Si substrate. (*i*) Surface topography, (*iii*) tip-contact current captured during the main PFT scan, and (*iii*) electrochemical current captured during the lift scan at a lift height of 150 nm. Areas denoted with 1–4 mark the location of individual nanoparticles (1–3) and nanoparticle cluster (4), respectively. Adapted with permission from Reference 99. Copyright 2017, Wiley-VCH. Abbreviations: AFM, atomic force microscopy; PFT, PeakForce Tapping; SECM, scanning electrochemical microscopy.

p-doped silicon and p^+-Si electrodes have been investigated with conductive AFM and PeakForce AFM-SECM measurements (99).

4.2. Biological Systems

AFM and specific AFM modes have long played a significant role in biorelated research. Because many processes in life sciences are associated with diffusional processes and redox chemistry, AFM-SECM could evolve into a key technique in these fields, particularly considering the breath of research published on biomedical research that uses conventional SECM as well as its associated issues of signal convolution (i.e., height and morphology) when operating on complex samples (e.g., cells, tissues, bacteria). Similar to its use in studying energy-related topics, AFM-SECM to date remains of limited use in life science research. One reason may be the complexity of the sample and the only very recent commercialization of SECM modules for AFM instruments. Early applications of AFM-SECM in the life science fields were targeted at mapping enzyme activity while simultaneously recording the topography of the structured enzyme-containing surfaces (88, 100).

A noteworthy excellent approach of Demaille and coworkers has been introduced in AFM-SECM, which is called molecule touching (Mt)/AFM-SECM (101), via the Tarm (33). In both methods, redox-active molecules are tethered to either the sample surface or the AFM-SECM tip, respectively. This circumvents any diffusional limitations in feedback mode imaging due to redox mediators that are freely available in bulk solution (101). Although this approach requires a labeling procedure, the authors showed remarkable examples of high-resolution topographical and electrochemical imaging (101–104). In terms of biomedically relevant applications, Mt/AFM-SECM was used to study end-grafted molecular layers of short ferrocene-labeled DNA chains in their single-stranded and double-stranded states (105). Using Mt/AFM-SECM, the distribution of proteins on individual virus particles could be imaged (102). From the topographical scans, isolated virus particles could be identified, whereas the simultaneously recorded current image

enabled mapping of the proteins selectively marked by redox antibodies. With this approach, a current detection sensitivity of ~10 fA and a spatial resolution of ~10 nm could be achieved, which allowed the detection of single-protein molecules at the extremity of isolated viruses (**Figure 6**). The potential of this approach was further demonstrated in a follow-up study in which the same group used Tarm/AFM-SECM to study the local reactivity of an electrochemically heterogeneous surface: HOPG and gold bands on silicon oxide (33). The multifunctional probe was shown to effectively shuttle electrons between the tip and substrate, where surface current maps showed clearly resolved step boundaries with a vertical resolution of 1 nm obtained in topography. The application of this technique for studying the kinetics of individual enzyme molecules could prove

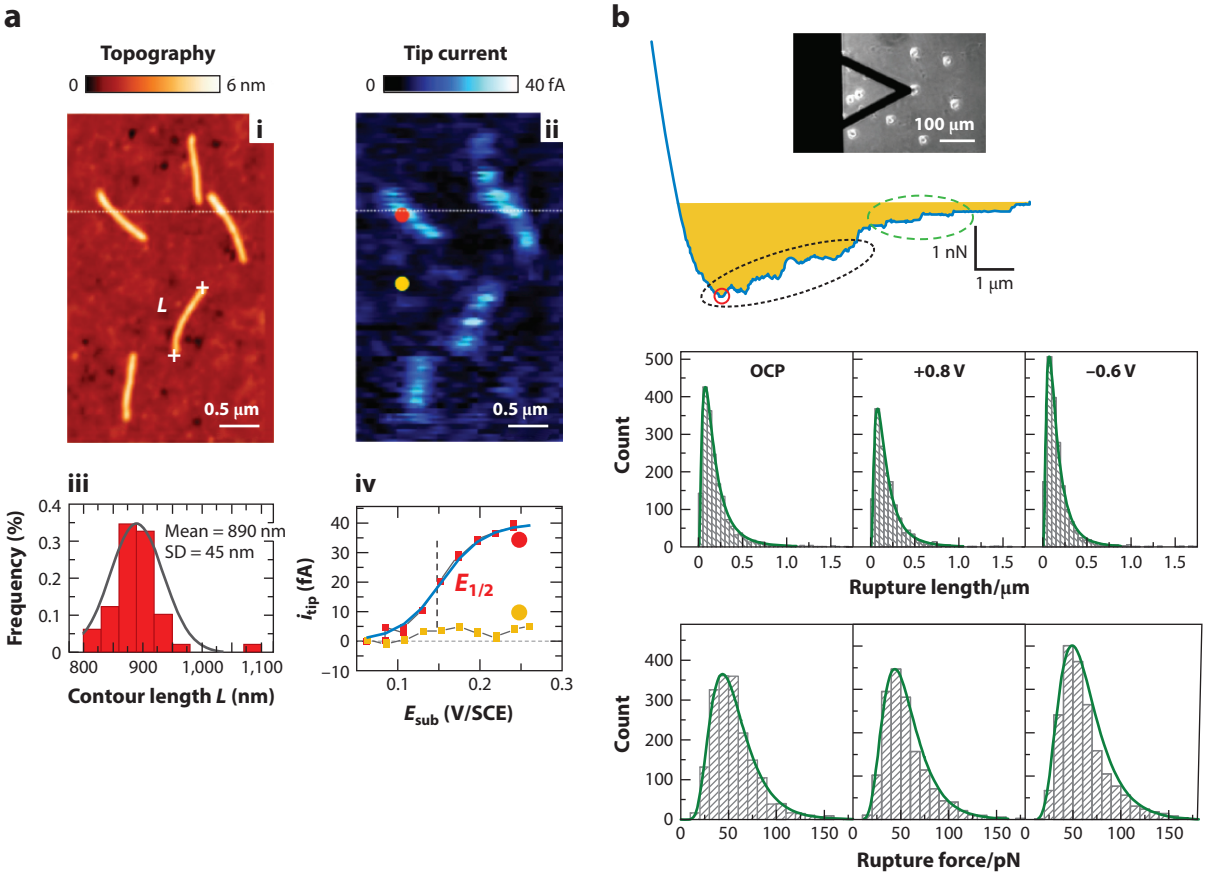

Figure 6

(*a*) Mt/AFM-SECM tapping mode imaging of coat protein–marked LMV particles immobilized on a gold substrate. Simultaneously acquired topography (*i*) and tip current (*ii*) images. The histogram in subpanel *iii* shows the distribution of the contour length of the virus particles shown in panel *a*. (*iv*) Dependence of the tip current i_{tip} with the substrate potential E_{sub}, with the i_{tip} measured either above a virus particle (*red dot* in *ii*, *iv*) or away from the viruses (*yellow dot* in *ii*, *iv*). Adapted with permission from Reference 102. Copyright 2015, American Chemical Society. (*b*) Force curve (retract part) obtained at OCP on a fibroblast: Green dashed line shows membrane tethers, red line denotes the maximum force, black dotted line indicates jumps, and the yellow shaded area reflects the obtained adhesion energy. Statistical data are shown in histograms for the different potentials (all versus Ag/AgCl) and force spectroscopic rupture data (membrane tethers). Histograms are fitted with log-normal functions to obtain peak distribution values (14 cells: 20 curves for each cell and potential). Adapted with permission from Reference 89. Copyright 2016, Royal Society of Chemistry. Abbreviations: LMV, lettuce mosaic virus; Mt, molecular touching mode; OCP, open circuit potential.

to be much more powerful than TREC. However, further reports of applications are rare, which may be associated with the complexity of the tip functionalization.

Although they have thus far only been used for cell force spectroscopic measurements, conductive colloidal AFM-SECM probes may have substantial potential for life cell measurements and biomedically relevant studies. Knittel et al. (89) used such probes for single-cell force measurements to investigate the adhesion properties of mouse fibroblasts with poly(3,4-ethylenedioxythiophene) doped with polystyrene sulfonate (PEDOT:PSS) as a function of the applied potential. Single-cell force spectroscopy is based on attaching a single cell onto a tipless AFM cantilever for quantification of single receptor binding, focal adhesion clusters, and whole cell adhesion (106). Due to limited viability of the attached cells, this approach is rather time consuming. With the polymer-modified colloidal probe, high-throughput measurements on multiple cells are possible under potential-induced changed properties of the polymer, thus improving the statistical sampling of cells without the need to remove the examined cells from their substrate. Conductive materials such as PEDOT:PSS are good scaffold materials because their properties such as conductivity, stiffness, and surface morphology can be tuned. Besides adhesion forces, information on such factors as oxygen consumption may also be obtained via electrochemical conversion. In the future, such probes may be employed, for example, in single-cell stimulation experiments, by locally releasing signal molecules, which subsequently may be analyzed in situ as well (e.g., release kinetics).

4.3. PeakForce Tapping

The potential of nanomechanical and electrochemical mapping was recently evaluated by performing AFM-SECM measurements in PFT mode. In PFT mode, which is derived from the pulsed-force mode, the probe is oscillated below its resonance frequency, with amplitudes ranging from less than 100 nm up to 3 μm at frequencies ranging from 0.25 to 2.0 kHz (107). Kranz and coworkers (54) showed the first combined PFT AFM-SECM measurements that imaged electrodes patterned onto soft polydimethylsiloxane (PDMS) substrates using AFM-SECM probes with recessed frame electrodes. As the tip was oscillated with a certain amplitude, the influence of the oscillating amplitude on the electrochemical contrast was investigated. The authors could also demonstrate that the individual microfabrication steps for patterning gold onto PDMS have significant influence on the Young's modulus. Nanomechanical AFM-SECM measurements were also applied by the same group to investigate the electrochemical and nanomechanical properties of gold nanoparticles (spherical and star-shaped) on conductive soft electrode materials such as carbon-doped PDMS. The physical and chemical properties of soft electrode materials strongly influence the interaction with factors such as biological components. The researchers showed that the electrochemical gold seed formation is located at areas with high carbon content, which could be visualized by changes in Young's modulus and deformation (108). Simultaneously recorded SECM feedback data also revealed the location of the nonstabilized gold nanoparticles. PFT AFM-SECM measurements were also performed at the single-nanoparticle level, thereby nicely demonstrating the current resolution limitations of this combined technique to image gold nanostar particles (79).

SECM measurements in combination with PFT mapping have also been shown with conical AFM-SECM probes (109, 110). A sub-100-nm spatial resolution for electrochemical imaging is reported on model substrates such as HOPG and a gold nanomesh electrode. With the electroactive area at the tip apex, measurements are performed in lift mode, when the topography scans are recorded by PFT. For the electrochemical measurement, the sinusoidal oscillation of the probe is turned off, and the current is recorded at a defined lift height, as shown in **Figure 7**. Nanomechanical adhesion data were only recorded for HOPG. As already

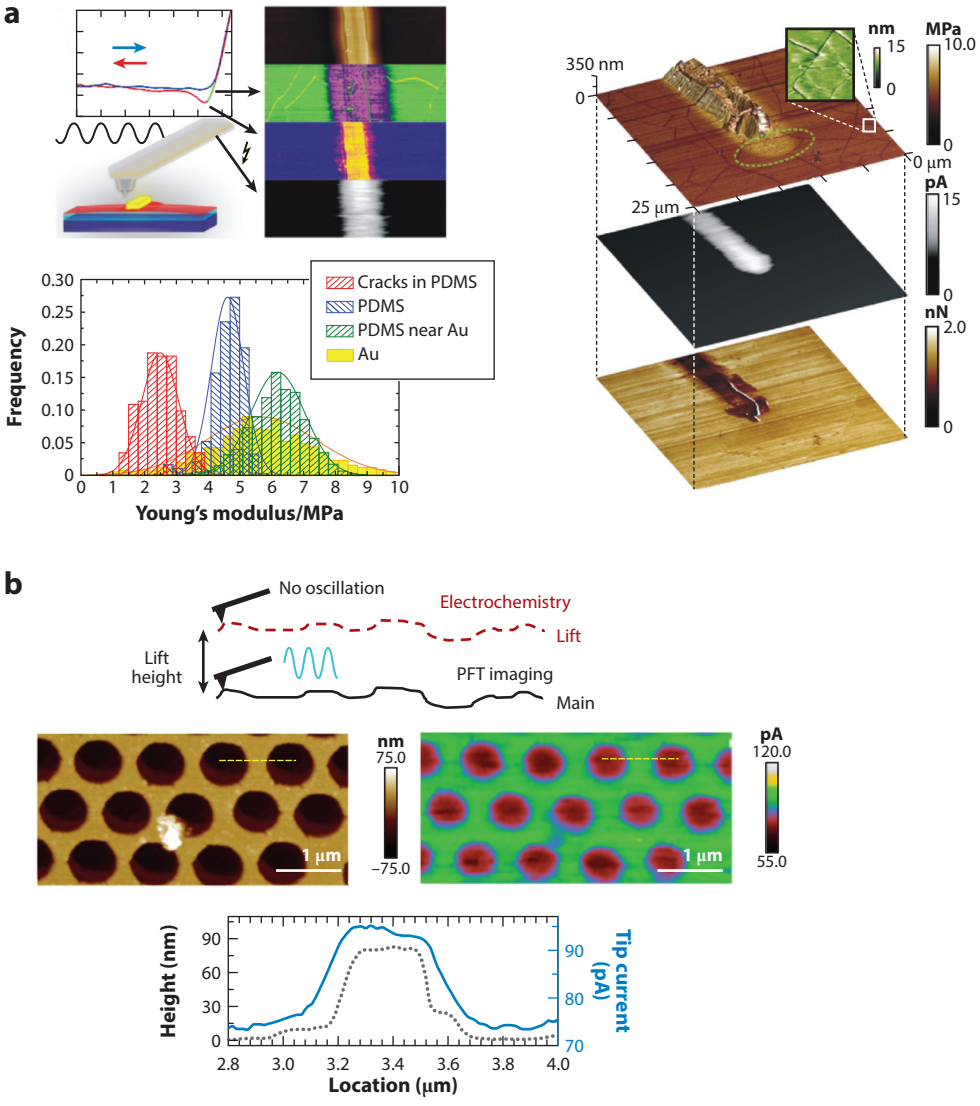

Figure 7

(*a*, *left*) Scheme of simultaneous nanomechanical and electrochemical mapping. (*a*, *right*) Measurement of a gold electrode patterned onto PDMS from top to bottom: three-dimensional topography of the structure overlaid with the Young's modulus (calculated with a DMT fit; green line shows increased stiffness of the PDMS surrounding the gold pattern; inset shows topography of the cracked PDMS). (*b*) Feedback-mode SECM image and tip–sample adhesion image. Adapted with permission from Reference 54. Copyright 2016, American Chemical Society. (*b*) Scheme of the interleaved scan mode and PFT-SECM image of a gold nanomesh. (*Left*) Surface topography shows a hole pattern of 0.75 × 1 µm. (*b*) Tip current captured from the lift scan at a lift height of 75 nm. Cross-sectional analysis of topography (*gray dotted line*) and tip current from lift scan (*solid blue line*) at locations indicated by the yellow dashed line in the images. Adapted with permission from Reference 110. Copyright 2017, IOP publishing. Abbreviations: DMT, Derjaguin-Muller-Toporov; PDMS, polydimethylsiloxane; PFT, PeakForce Tapping; SECM, scanning electrochemical microscopy.

mentioned, nanomechanical-electrochemical mapping has substantial potential for measurements involving aging processes, which influence the physical properties such as Young's modulus and adhesion, but they may also have an effect on the activity of the surface. This may then be detected simultaneously or sequentially with the electrochemical measurements, depending on the probe design. In combination with detailed theoretical modeling, this may further expand our fundamental understanding of molecular processes in complex heterogeneous samples.

5. CONCLUDING REMARKS

High-resolution imaging based on multifunctional AFM contributes to fundamental understanding of molecular processes, particularly when performed under in situ conditions or when imaging live cells or heterogeneous interfaces. Although the methods presented in this review still have to be considered as highly specialized techniques applied only by a small research community, recent developments and protocols for reliable AFM probe functionalization as well as commercially available bifunctional probes and add-on modules for existing instrumentation will hopefully result in their application by a broader group of researchers in the near future. For AFM-SECM, exciting applications in catalysis and biomedically relevant fields will also hopefully be developed. It should be noted that both AFM-SECM probe designs have their specific advantages and drawbacks in respect to achievable resolution but also in terms of probe modification of imaging sensors and imaging modes (e.g., simultaneous recording or sequential data recording). In our opinion, it is desirable to have a diversity of designs fulfilling the needs and requirements for the specific scientific challenge.

DISCLOSURE STATEMENT

The authors are not aware of any affiliations, memberships, funding, or financial holdings that might be perceived as affecting the objectivity of this review.

ACKNOWLEDGMENTS

Parts of the research presented in this review were supported by the Deutscher Akademischer Austauschdienst (DAAD; Berlin, Germany) and by the Deutsche Forschungesgemeinschaft (DFG) (research grant GRK2203-PULMOSENS).

LITERATURE CITED

1. Eifert A, Kranz C. 2014. Hyphenating atomic force microscopy. *Anal. Chem.* 86(11):5190–200
2. Binnig G, Quate CF, Gerber C. 1986. Atomic force microscope. *Phys. Rev. Lett.* 56:930–33
3. Florin EL, Moy VT, Gaub HE. 1994. Adhesion forces between individual ligand-receptor pairs. *Science* 264(5157):415–17
4. Frisbie CD, Rozsnyai LF, Noy A, Wrighton MS, Lieber CM. 1994. Functional-group imaging by chemical force microscopy. *Science* 265(5181):2071–74
5. Noy A, Frisbie CD, Rozsnyai LF, Wrighton MS, Lieber CM. 1995. Chemical force microscopy: exploiting chemically-modified tips to quantify adhesion, friction, and functional group distributions in molecular assemblies. *J. Am. Chem. Soc.* 117(30):7943–51
6. Gross L, Wang ZL, Ugarte D, Mohn F, Moll N, et al. 2009. The chemical structure of a molecule resolved by atomic force microscopy. *Science* 325(5994):1110–14
7. Gross L, Mohn F, Moll N, Meyer G, Ebel R, et al. 2010. Organic structure determination using atomic-resolution scanning probe microscopy. *Nat. Chem.* 2(10):821–25

8. Gross L. 2011. Recent advances in submolecular resolution with scanning probe microscopy. *Nat. Chem.* 3(4):273–78
9. Pavliček N, Gross L. 2017. Generation, manipulation and characterization of molecules by atomic force microscopy. *Nat. Rev. Chem.* 1(1):0005
10. Hinterdorfer P, Garcia-Parajo MF, Dufrêne YF. 2012. Single-molecule imaging of cell surfaces using near-field nanoscopy. *Acc. Chem. Res.* 45(3):327–36
11. Senapati S, Lindsay S. 2016. Recent progress in molecular recognition imaging using atomic force microscopy. *Acc. Chem. Res.* 49(3):503–10
12. Alsteens D, Müller DJ, Dufrêne YF. 2017. Multiparametric atomic force microscopy imaging of biomolecular and cellular systems. *Acc. Chem. Res.* 50(4):924–31
13. Dufrêne YF, Ando T, Garcia R, Alsteens D, Martinez-Martin D, et al. 2017. Imaging modes of atomic force microscopy for application in molecular and cell biology. *Nat. Nanotechnol.* 12(4):295–307
14. Helenius J, Heisenberg C-P, Gaub HE, Müller DJ. 2008. Single-cell force spectroscopy. *J. Cell Sci.* 121(11):1785–91
15. Butt H-J, Cappella B, Kappl M. 2005. Force measurements with the atomic force microscope: Technique, interpretation and applications. *Surf. Sci. Rep.* 59(1–6):1–152
16. Hughes ML, Dougan L. 2016. The physics of pulling polyproteins: a review of single molecule force spectroscopy using the AFM to study protein unfolding. *Rep. Prog. Phys.* 79(7):76601
17. Pittenger B, Erina N, Su C. 2011. *Quantitative mechanical property mapping at the nanoscale with PeakForce QNM*. Appl. Note 128, Bruker Corp., Fremont, Calif.
18. Rosa-Zeiser A, Weilandt E, Hild S, Marti O. 1997. The simultaneous measurement of elastic, electrostatic and adhesive properties by scanning force microscopy: pulsed-force mode operation. *Meas. Sci. Technol.* 8(11):1333–38
19. Gaboriaud F, Parcha BS, Gee ML, Holden JA, Strugnell RA. 2008. Spatially resolved force spectroscopy of bacterial surfaces using force-volume imaging. *Coll. Surf. B Biointerfaces* 62(2):206–13
20. Medalsy I, Hensen U, Müller DJ. 2011. Imaging and quantifying chemical and physical properties of native proteins at molecular resolution by force-volume AFM. *Angew. Chem. Int. Ed.* 50(50):12103–8
21. Pfreundschuh M, Alsteens D, Hilbert M, Steinmetz MO, Müller DJ. 2014. Localizing chemical groups while imaging single native proteins by high-resolution atomic force microscopy. *Nano Lett.* 14(5):2957–64
22. Wegmann S, Medalsy ID, Mandelkow E, Müller DJ. 2013. The fuzzy coat of pathological human Tau fibrils is a two-layered polyelectrolyte brush. *PNAS* 110(4):E313–21
23. Alsteens D, Pfreundschuh M, Zhang C, Spoerri PM, Coughlin SR, et al. 2015. Imaging G protein-coupled receptors while quantifying their ligand-binding free-energy landscape. *Nat. Methods* 12(9):845–51
24. Alsteens D, Newton R, Schubert R, Martinez-Martin D, Delguste M, et al. 2017. Nanomechanical mapping of first binding steps of a virus to animal cells. *Nat. Nanotechnol.* 12(2):177–83
25. Formosa-Dague C, Speziale P, Foster TJ, Geoghegan JA, Dufrêne YF. 2016. Zinc-dependent mechanical properties of *Staphylococcus aureus* biofilm-forming surface protein SasG. *PNAS* 113(2):410–15
26. Alsteens D, Trabelsi H, Soumillion P, Dufrêne YF. 2013. Multiparametric atomic force microscopy imaging of single bacteriophages extruding from living bacteria. *Nat. Commun.* 4:2926
27. Riener CK, Kienberger F, Hahn CD, Buchinger GM, Egwim IOC, et al. 2003. Heterobifunctional crosslinkers for tethering single ligand molecules to scanning probes. *Anal. Chim. Acta* 497(1–2):101–14
28. Manna S, Senapati S, Lindsay S, Zhang P. 2015. A three-arm scaffold carrying affinity molecules for multiplex recognition imaging by atomic force microscopy: the synthesis, attachment to silicon tips, and detection of proteins. *J. Am. Chem. Soc.* 137(23):7415–23
29. Lohr D, Bash R, Wang H, Yodh J, Lindsay S. 2007. Using atomic force microscopy to study chromatin structure and nucleosome remodeling. *Methods* 41(3):333–41
30. Riener CK, Stroh CM, Ebner A, Klampfl C, Gall AA, et al. 2003. Simple test system for single molecule recognition force microscopy. *Anal. Chim. Acta* 479(1):59–75
31. Martines E, Zhong J, Muzard J, Lee AC, Akhremitchev BB, et al. 2012. Single-molecule force spectroscopy of the *Aplysia* cell adhesion molecule reveals two homophilic bonds. *Biophys. J.* 103(4):649–57

32. Klein DC, Øvrebø KM, Latz E, Espevik T, Stokke BT. 2012. Direct measurement of the interaction force between immunostimulatory CpG-DNA and TLR9 fusion protein. *J. Mol. Recognit.* 25(2):74–81
33. Anne A, Cambril E, Chovin A, Demaille C, Goyer C. 2009. Electrochemical atomic force mediator for topographic and functional imaging of nanosystems. *ACS Nano* 3(10):2927–40
34. Preiner J, Ebner A, Chtcheglova L, Zhu R, Hinterdorfer P. 2009. Simultaneous topography and recognition imaging: physical aspects and optimal imaging conditions. *Nanotechnology* 20(21):215103
35. Han W, Lindsay SM, Jing T. 1996. A magnetically driven oscillating probe microscope for operation in liquids. *Appl. Phys. Lett.* 69(26):4111–13
36. Raab A, Han W, Badt D, Smith-Gill SJ, Lindsay SM, et al. 1999. Antibody recognition imaging by force microscopy. *Nat. Biotechnol.* 17(9):901–5
37. Lin L, Wang H, Liu Y, Yan H, Lindsay S. 2006. Recognition imaging with a DNA aptamer. *Biophys. J.* 90(11):4236–38
38. Senapati S, Manna S, Lindsay S, Zhang P. 2013. Application of catalyst-free click reactions in attaching affinity molecules to tips of atomic force microscopy for detection of protein biomarkers. *Langmuir* 29(47):14622–30
39. Hinterdorfer P, Baumgartner W, Gruber HJ, Schilcher K, Schindler H. 1996. Detection and localization of individual antibody-antigen recognition events by atomic force microscopy. *PNAS* 93(8):3477–81
40. Stroh C, Wang H, Bash R, Ashcroft B, Nelson J, et al. 2004. Single-molecule recognition imaging microscopy. *PNAS* 101(34):12503–7
41. Lin L, Hom D, Lindsay SM, Chaput JC. 2007. In vitro selection of histone H4 aptamers for recognition imaging microscopy. *J. Am. Chem. Soc.* 129(47):14568–69
42. Bard AJ, Fu-Ren FF, Kwak J, Lev O. 1989. Scanning electrochemical microscopy. Introduction and principles. *Anal. Chem.* 61:132–38
43. Polcari D, Dauphin-Ducharme P, Mauzeroll J. 2016. Scanning electrochemical microscopy: a comprehensive review of experimental parameters from 1989 to 2015. *Chem. Rev.* 116(22):13234–78
44. Mirkin MV, Sun T, Yu Y, Zhou M. 2016. Electrochemistry at one nanoparticle. *Acc. Chem. Res.* 49(10):2328–35
45. Kang M, Momotenko D, Page A, Perry D, Unwin PR. 2016. Frontiers in nanoscale electrochemical imaging: faster, multifunctional, and ultrasensitive. *Langmuir* 32(32):7993–8008
46. Ballesteros Katemann B, Schulte A, Schuhmann W. 2003. Constant-distance mode scanning electrochemical microscopy (SECM)–Part I: adaptation of a non-optical shear-force-based positioning mode for SECM tips. *Chem. Eur. J.* 9(9):2025–33
47. Ballesteros Katemann B, Schulte A, Schuhmann W. 2004. Constant-distance mode scanning electrochemical microscopy. Part II: high-resolution SECM imaging employing Pt nanoelectrodes as miniaturized scanning probes. *Electroanalysis* 16(12):60–65
48. Takahashi Y, Shevchuk AI, Novak P, Zhang Y, Ebejer N, et al. 2011. Multifunctional nanoprobes for nanoscale chemical imaging and localized chemical delivery at surfaces and interfaces. *Angew. Chem. Int. Ed.* 50(41):9638–42
49. Comstock DJ, Elam JW, Pellin MJ, Hersam MC. 2010. Integrated ultramicroelectrode- nanopipet probe for concurrent scanning electrochemical microscopy and scanning ion conductance microscopy. *Anal. Chem.* 82:1270–76
50. Ebejer N, Güell AG, Lai SCS, McKelvey K, Snowden ME, Unwin PR. 2013. Scanning electrochemical cell microscopy: a versatile technique for nanoscale electrochemistry and functional imaging. *Annu. Rev. Anal. Chem.* 6:329–51
51. Macpherson JV, Unwin PR. 2000. Combined scanning electrochemical–atomic force microscopy. *Anal. Chem.* 72(2):276–85
52. Macpherson JV, Unwin PR. 2001. Noncontact electrochemical imaging with combined scanning electrochemical atomic force microscopy. *Anal. Chem.* 73(3):550–57
53. Kranz C, Friedbacher G, Mizaikoff B, Lugstein A, Smoliner J, Bertagnolli E. 2001. Integrating an ultramicroelectrode in an AFM cantilever: combined technology for enhanced information. *Anal. Chem.* 73:2491–500

54. Knittel P, Mizaikoff B, Kranz C. 2016. Simultaneous nanomechanical and electrochemical mapping: combining peak force tapping atomic force microscopy with scanning electrochemical microscopy. *Anal. Chem.* 88(12):6174–78
55. Ghorbal A, Grisotto F, Charlier J, Palacin S, Goyer C, et al. 2013. Nano-electrochemistry and nano-electrografting with an original combined AFM-SECM. *Nanomaterials* 3(2):303–16
56. Izquierdo J, Eifert A, Souto RM, Kranz C. 2015. Simultaneous pit generation and visualization of pit topography using combined atomic force-scanning electrochemical microscopy. *Electrochem. Commun.* 51:15–18
57. Davoodi A, Pan J, Leygraf C, Norgren S. 2008. The role of intermetallic particles in localized corrosion of an aluminum alloy studied by SKPFM and integrated AFM/SECM. *J. Electrochem. Soc.* 155(5):C211–18
58. Burt DP, Wilson NR, Janus U, Macpherson JV, Unwin PR. 2008. In-situ atomic force microscopy (AFM) imaging: influence of AFM probe geometry on diffusion to microscopic surfaces. *Langmuir* 24(22):12867–76
59. Izquierdo J, Fernández-Pérez BM, Eifert A, Souto RM, Kranz C. 2016. Simultaneous atomic force–scanning electrochemical microscopy (AFM-SECM) imaging of copper dissolution. *Electrochim. Acta* 201:320–32
60. Eckhard K, Shin H, Mizaikoff B, Schuhmann W, Kranz C. 2007. Alternating current (AC) impedance imaging with combined atomic force scanning electrochemical microscopy (AFM-SECM). *Electrochem. Commun.* 9(6):1311–15
61. Eckhard K, Kranz C, Shin H, Mizaikoff B, Schuhmann W. 2007. Frequency dependence of the electrochemical activity contrast in AC-scanning electrochemical microscopy and atomic force microscopy-AC-scanning electrochemical microscopy imaging. *Anal. Chem.* 79(14):5435–38
62. Shin H, Hesketh PJ, Mizaikoff B, Kranz C. 2007. Batch fabrication of atomic force microscopy probes with recessed integrated ring microelectrodes at a wafer level. *Anal. Chem.* 79(13):4769–77
63. Eckhard K, Chen X, Turcu F, Schuhmann W. 2006. Redox competition mode of scanning electrochemical microscopy (RC-SECM) for visualisation of local catalytic activity. *Phys. Chem. Chem. Phys.* 8(45):5359–65
64. Velmurugan J, Agrawal A, An S, Choudhary E, Szalai VA. 2017. Fabrication of scanning electrochemical microscopy-atomic force microscopy probes to image surface topography and reactivity at the nanoscale. *Anal. Chem.* 89(5):2687–91
65. KeySight Tech. *N9545F SECM (scanning electrochemical microscopy)*. Keysight Tech., Böblingen, Ger. **https://www.keysight.com/en/pd-2417461-pn-N9545F/secm-scanning-electrochemical-microscopy?cc=US&lc=eng**
66. Bruker Corp. *PeakForce SECM*. Bruker Corp., Fremont, CA. **https://www.bruker.com/products/surface-and-dimensional-analysis/atomic-force-microscopes/modes/modes/imaging-modes/peakforce-secm/overview.html**
67. Abbou J, Demaille C, Druet M, Moiroux J. 2002. Fabrication of submicrometer-sized gold electrodes of controlled geometry for scanning electrochemical-atomic force microscopy. *Anal. Chem.* 74(6):1627–34
68. Dobson PS, Weaver JMR, Holder MN, Unwin PR, Macpherson JV. 2005. Characterization of batch-microfabricated scanning electrochemical-atomic force microscopy probes. *Anal. Chem.* 77:424–33
69. Gullo MR, Frederix PLTM, Akiyama T, Engel A, DeRooij NF, Staufer U. 2006. Characterization of microfabricated probes for combined atomic force and high-resolution scanning electrochemical microscopy. *Anal. Chem.* 78(15):5436–42
70. Shin H, Hesketh PJ, Mizaikoff B, Kranz C. 2008. Development of wafer-level batch fabrication for combined atomic force-scanning electrochemical microscopy (AFM-SECM) probes. *Sens. Actuators B Chem.* 134(2):488–95
71. Salomo M, Pust SE, Wittstock G, Oesterschulze E. 2010. Integrated cantilever probes for SECM/AFM characterization of surfaces. *Microelectron. Eng.* 87(5–8):1537–39
72. Heintz ELH, Kranz C, Mizaikoff B, Noh HS, Hesketh P, et al. 2001. Characterization of Parylene coated combined scanning probe tips for in-situ electrochemical and topographical imaging. *Proc. IEEE Conf. Nanotechnol.* 346–51
73. Derylo MA, Morton KC, Baker LA. 2011. Parylene insulated probes for scanning electrochemical-atomic force microscopy. *Langmuir* 27(22):13925–30

74. Davoodi A, Pan J, Leygraf C, Norgren S. 2005. In situ investigation of localized corrosion of aluminum alloys in chloride solution using integrated EC-AFM/SECM techniques. *Electrochem. Solid-State Lett.* 8(6):B21–24
75. Eifert A, Smirnov W, Frittmann S, Nebel C, Mizaikoff B, Kranz C. 2012. Atomic force microscopy probes with integrated boron doped diamond electrodes: fabrication and application. *Electrochem. Commun.* 25:30–34
76. Eifert A, Mizaikoff B, Kranz C. 2015. Advanced fabrication process for combined atomic force-scanning electrochemical microscopy (AFM-SECM) probes. *Micron* 68:27–35
77. Wiedemair J, Moon J-S, Reinauer F, Mizaikoff B, Kranz C. 2010. Ion beam induced deposition of platinum carbon composite electrodes for combined atomic force microscopy-scanning electrochemical microscopy. *Electrochem. Commun.* 12(7):989–91
78. Knittel P, Higgins MJ, Kranz C. 2014. Nanoscopic polypyrrole AFM-SECM probes enabling force measurements under potential control. *Nanoscale* 6(4):2255–60
79. Knittel P, Bibikova O, Kranz C. 2016. Challenges in nanoelectrochemical and nanomechanical studies of individual anisotropic gold nanoparticles. *Faraday Discuss.* 193:353–69
80. Rodriguez RD, Anne A, Cambril E, Demaille C. 2011. Optimized hand fabricated AFM probes for simultaneous topographical and electrochemical tapping mode imaging. *Ultramicroscopy* 111(8):973–81
81. Tefashe UM, Wittstock G. 2013. Quantitative characterization of shear force regulation for scanning electrochemical microscopy. *Comptes Rendus Chim.* 16(1):7–14
82. Anne A, Demaille C, Goyer C. 2009. Electrochemical atomic-force microscopy using a tip-attached redox mediator. Proof-of-concept and perspectives for functional probing of nanosystems. *ACS Nano* 3(4):819–27
83. Kurzawa C, Hengstenberg A, Schuhmann W. 2002. Immobilization method for the preparation of biosensors based on pH shift-induced deposition of biomolecule-containing polymer films. *Anal. Chem.* 74(2):355–61
84. Kueng A, Kranz C, Mizaikoff B. 2004. Amperometric ATP biosensor based on polymer entrapped enzymes. *Biosens. Bioelectron.* 19(10):1301–7
85. Andronescu C, Pöller S, Schuhmann W. 2014. Electrochemically induced deposition of poly(benzoxazine) precursors as immobilization matrix for enzymes. *Electrochem. Commun.* 41:12–15
86. Ziller C, Lin J, Knittel P, Friedrich L, Andronescu C, et al. 2017. Poly(benzoxazine) as an immobilization matrix for miniaturized ATP and glucose biosensors. *ChemElectroChem* 4(4):864–71
87. Kueng A, Kranz C, Lugstein A, Bertagnolli E, Mizaikoff B. 2005. AFM-tip-integrated amperometric microbiosensors: high-resolution imaging of membrane transport. *Angew. Chem. Int. Ed.* 44(22):3419–22
88. Kranz C, Kueng A, Lugstein A, Bertagnolli E, Mizaikoff B. 2004. Mapping of enzyme activity by detection of enzymatic products during AFM imaging with integrated SECM-AFM probes. *Ultramicroscopy* 100(3–4):127–34
89. Knittel P, Zhang H, Kranz C, Wallace GG, Higgins MJ. 2016. Probing the PEDOT:PSS/cell interface with conductive colloidal probe AFM-SECM. *Nanoscale* 8:4475–81
90. Sklyar O, Kueng A, Kranz C, Mizaikoff B, Lugstein A, et al. 2005. Numerical simulation of scanning electrochemical microscopy experiments with frame-shaped integrated atomic force microscopy-SECM probes using the boundary element method analyzed for a model substrate containing pronounced. *Anal. Chem.* 77(3):764–71
91. Pust SE, Salomo M, Oesterschulze E, Wittstock G. 2010. Influence of electrode size and geometry on electrochemical experiments with combined SECM-SFM probes. *Nanotechnology* 21(10):105709
92. Leonhardt K, Avdic A, Lugstein A, Pobelov I, Wandlowski T, et al. 2013. Scanning electrochemical microscopy: diffusion controlled approach curves for conical AFM-SECM tips. *Electrochem. Commun.* 27:29–33
93. Smirnov W, Kriele A, Hoffmann R, Sillero E, Hees J, et al. 2011. Diamond-modified AFM probes: from diamond nanowires to atomic force microscopy-integrated boron-doped diamond electrodes. *Anal. Chem.* 83:4936–41
94. Davoodi A, Farzadi A, Pan J, Leygraf C, Zhu Y. 2008. Developing an AFM-based SECM system; instrumental setup, SECM simulation, characterization, and calibration. *J. Electrochem. Soc.* 155(8):C474–85

95. Izquierdo J, Eifert A, Kranz C, Souto RM. 2017. In situ investigation of copper corrosion in acidic chloride solution using atomic force–scanning electrochemical microscopy. *Electrochim. Acta* 247:588–99
96. Izquierdo J, Eifert A, Kranz C, Souto RM. 2015. In situ monitoring of pit nucleation and growth at an iron passive oxide layer by using combined atomic force and scanning electrochemical microscopy. *ChemElectroChem* 2(11):1847–56
97. Macpherson JV, Gueneau de Mussy J-P, Delplancke J-L. 2002. High-resolution electrochemical, electrical, and structural characterization of a dimensionally stable $Ti/TiO_2/Pt$ electrode. *J. Electrochem. Soc.* 149(7):B306–13
98. Zampardi G, Klink S, Kuznetsov V, Erichsen T, Maljusch A, et al. 2015. Combined AFM/SECM investigation of the solid electrolyte interphase in Li-ion batteries. *ChemElectroChem* 2(10):1607–11
99. Jiang J, Huang Z, Xiang C, Poddar R, Lewerenz H-J, et al. 2017. Nanoelectrical and nanoelectrochemical imaging of Pt/p-Si and Pt/p^+-Si electrodes. *ChemSusChem* 10(22):4657–63
100. Kueng A, Kranz C, Lugstein A, Bertagnolli E, Mizaikoff B. 2003. Integrated AFM-SECM in tapping mode: simultaneous topographical and electrochemical imaging of enzyme activity. *Angew. Chem. Int. Ed.* 42(28):3238–40
101. Anne A, Cambril E, Chovin A, Demaille C. 2010. Touching surface-attached molecules with a microelectrode: mapping the distribution of redox-labeled macromolecules by electrochemical-atomic force microscopy. *Anal. Chem.* 82(15):6353–62
102. Nault L, Taofifenua C, Anne A, Chovin A, Demaille C, et al. 2015. Electrochemical atomic force microscopy imaging of redox-immunomarked proteins on native potyviruses: from subparticle to single-protein resolution. *ACS Nano* 9(5):4911–24
103. Anne A, Chovin A, Demaille C, Lafouresse M. 2011. High-resolution mapping of redox-immunomarked proteins using electrochemical-atomic force microscopy in molecule touching mode. *Anal. Chem.* 83(20):7924–32
104. Anne A, Bahri MA, Chovin A, Demaille C, Taofifenua C. 2014. Probing the conformation and 2D-distribution of pyrene-terminated redox-labeled poly(ethylene glycol) chains end-adsorbed on HOPG using cyclic voltammetry and atomic force electrochemical microscopy. *Phys. Chem. Chem. Phys.* 16(10):4642–52
105. Wang K, Goyer C, Anne A, Demaille C. 2007. Exploring the motional dynamics of end-grafted DNA oligonucleotides by in situ electrochemical atomic force microscopy. *J. Phys. Chem. B.* 111(21):6051–58
106. Benoit M, Gabriel D, Gerisch G, Gaub HE. 2000. Discrete interactions in cell adhesion measured by single-molecule force spectroscopy. *Nat. Cell Biol.* 2(6):313–17
107. Minne S, Hu Y, Hu S, Pittenger B, Su C. 2010. Nanoscale quantitative mechanical property mapping using peak force tapping atomic force microscopy. *Microsc. Microanal.* 16(Suppl. 2):464–65
108. Guin SK, Knittel P, Daboss S, Breusow A, Kranz C. 2017. Template- and additive-free electrosynthesis and characterization of spherical gold nanoparticles on hydrophobic conducting polydimethylsiloxane. *Chemistry* 12(13):1615–24
109. Huang Z, Wolf P DE, Poddar R, Li C, Mark A, et al. 2016. PeakForce scanning electrochemical microscopy with nanoelectrode probes. *Microsc. Today* 24:18–25
110. Nellist MR, Chen Y, Mark A, Gödrich S, Stelling C, et al. 2017. Atomic force microscopy with nanoelectrode tips for high resolution electrochemical, nanoadhesion and nanoelectrical imaging. *Nanotechnology* 28(9):95711

Annual Review of
Analytical Chemistry

Volume 11, 2018

Contents

Errata

An online log of corrections to *Annual Review of Analytical Chemistry* articles may be found at http://www.annualreviews.org/errata/anchem